Inorganic Chemistry

Article

pubs.acs.org/IC

Addressing the Chemical Sorcery of "GaI": Benefits of Solid-State Analysis Aiding in the Synthesis of P→Ga Coordination Compounds

Brian J. Malbrecht, Jonathan W. Dube, Mathew J. Willans, and Paul J. Ragogna*

The Department of Chemistry and The Centre for Advanced Materials and Biomaterials Research (CAMBR), The University of Western Ontario, 1151 Richmond Street, London, Ontario N6A 5B7, Canada

Supporting Information

ABSTRACT: The differing structures and reactivities of "GaI" samples prepared with different reaction times have been investigated in detail. Analysis by FT-Raman spectroscopy, powder X-ray diffraction, ^{71}Ga solid-state NMR spectroscopy, and ^{127}I nuclear quadrupole resonance (NQR) provides concrete evidence for the structure of each "GaI" sample prepared. These techniques are widely accessible and can be implemented quickly and easily to identify the nature of the "GaI" in hand. The "GaI" prepared from exhaustive reaction times (100 min) is shown to possess Ga_2I_3 and an overall formula of $[Ga^0]_2[Ga^+]_2[Ga_2I_6^{2-}]$, while the "GaI" prepared with the shortest reaction time (40 min) contains GaI_2 and has the overall formula $[Ga^0]_2[Ga^+][GaI_4^-]$. Intermediate "GaI" samples were consistently shown to be fractionally composed of each of these two preceding formulations and no other distinguishable phases. These "GaI" phases were then shown to give unique products upon reactions with the anionic bis(phosphino)borate ligand class. The reaction of the early-phase "GaI" gives rise to a unique phosphine Ga(II) dimeric coordination compound (**3**), which was isolated reproducibly in 48% yield and convincingly characterized. A base-stabilized GaI→GaI_3 fragment (**4**) was also isolated using the late-phase "GaI" and characterized by multinuclear NMR spectroscopy and X-ray crystallography. These compounds can be considered unique examples of low-oxidation-state P→Ga coordination compounds and possess relatively long Ga−P bond lengths in the solid-state structures. The anionic borate backbone therefore results in interesting architectures about gallium that have not been observed with neutral phosphines.

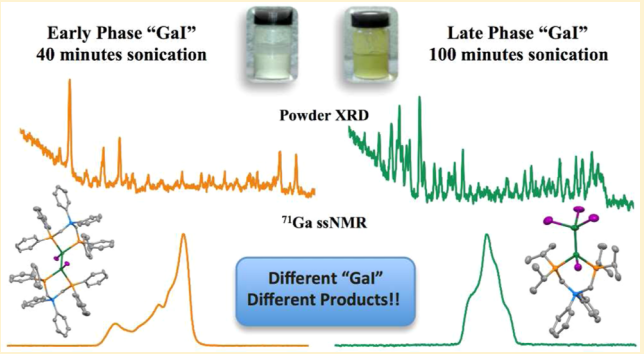

INTRODUCTION

Modern research in synthetic main-group chemistry frequently focuses on the synthesis of compounds that possess multiple bonds or are coordinatively unsaturated. Many of the resulting coordination complexes have been shown to possess the coordination space and accessible electronic structure that allows them to perform roles traditionally associated with transition metals.[1,2] The synthesis of low-valent gallium complexes is interesting for their unusual bonding environments (**A**; Figure 1) and for their potential in bond activation and catalysis. To this end, N-heterocyclic Ga(I) compounds (**B**, **C**) have been synthesized and shown to serve as suitable ligands for both p- and d-block elements.[3−14] The structure and bonding of a unique series of base-stabilized cationic gallium(I) compounds have also been recently reported by Krossing and co-workers (**D**).[15−20] Ga(II) complexes typically feature a Ga−Ga bond, and one dimer in particular (**E**) has been shown to catalyze the hydroamination of phenylacetylene.[21,22] This reactivity constitutes a rare example of an organic C−N bond forming reaction catalyzed by a purely main group coordination compound and highlights the potential of low-valent gallium compounds to have an effect beyond the field of coordination chemistry.[23,24]

In most cases, the synthesis of low-valent gallium compounds begins with the Ga(I) synthon "GaI".[25] While the synthesis of "GaI" has been well established,[26,27] there has been some recent debate regarding the true composition of this reagent. A report by Coban has been commonly cited as assigning "GaI" to have the dominant composition Ga_2I_3 (in the solid state: $[Ga^+]_2[Ga_2I_6]^{2-}$) with the possible presence of other gallium subiodides.[28] However, this report is inaccessible, which makes data comparisons and analysis impossible. Contradicting the Coban proposal is a solid-state NMR (ssNMR) investigation by Bryce and co-workers which has recently suggested that "GaI" is best assigned as $[Ga^0]_2[Ga]^+[GaI_4]^-$ (where $[Ga]^+[GaI_4]^-$ is also described as GaI_2).[29] To attempt to resolve this discrepancy and to provide the necessary data for standardization of the "GaI" synthesis across different laboratories, we undertook a full characterization of "GaI" samples at several different stages of its preparation. Analysis by numerous techniques—including FT-Raman spectroscopy, ^{71}Ga solid-state NMR spectroscopy (ssNMR), ^{127}I nuclear quadrupole resonance (NQR), and powder X-ray diffraction (pXRD)—

Received: May 15, 2014
Published: September 3, 2014

   dx.doi.org/10.1021/ic501139w | Inorg. Chem. 2014, 53, 9644−9656

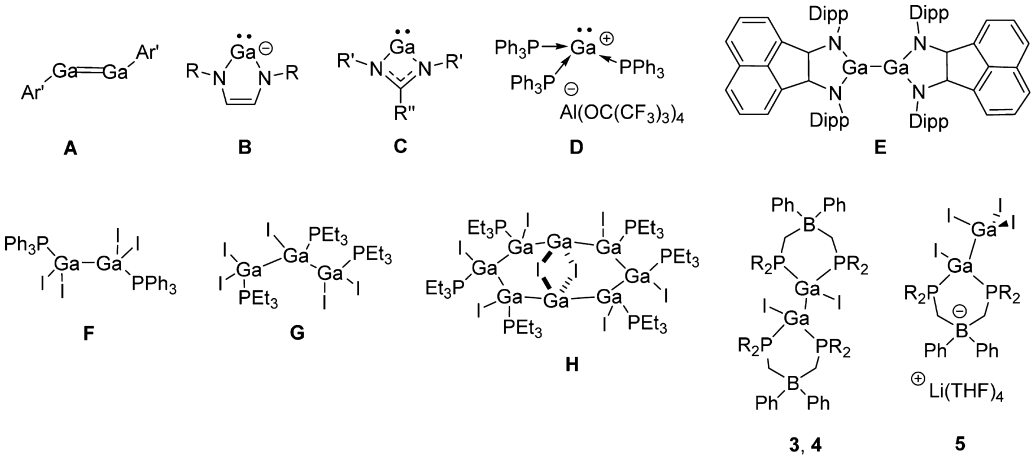

Figure 1. Selection of neutral and charged low-valent gallium(I) compounds (**A**–**D**), a gallium(II) compound that catalyzes hydroamination reactions (**E**), gallium–phosphine coordination compounds isolated from "GaI" (**F**–**H**), and compounds reported in this work (**3**–**5**).

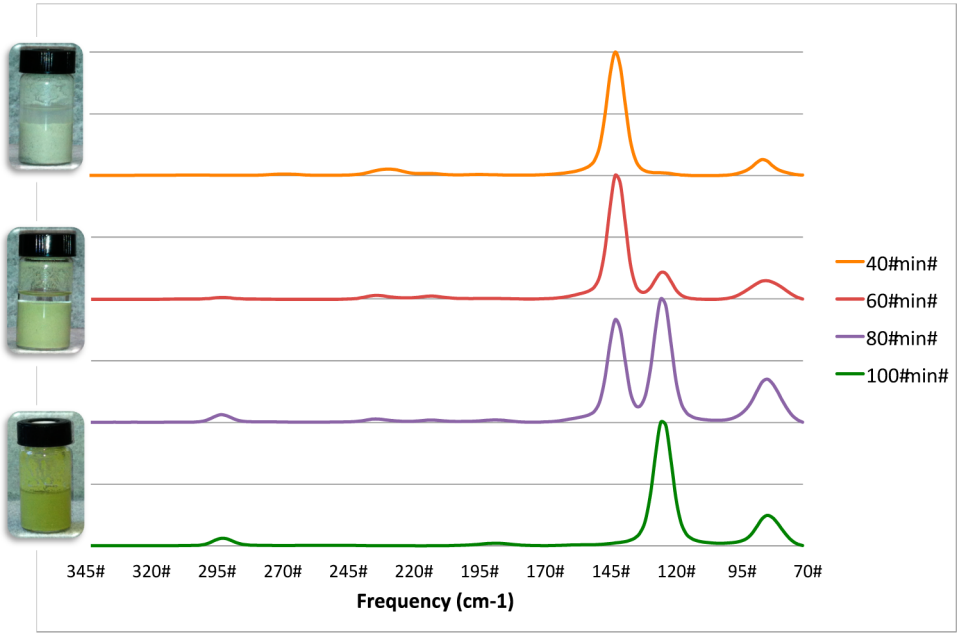

Figure 2. Raman spectra of "GaI" as a function of reaction time: from top to bottom 40, 60, 80, and 100 min. Insets show toluene suspensions of the "GaI" solids that correspond to the Raman spectra.

revealed that "GaI" can be *controllably* synthesized in two different phases. An "early" gray phase is the first to be formed during synthesis of "GaI", followed by a "late" green phase that represents the true end point of the "GaI" synthesis. Intermediate phases containing a mixture of the early and late phases were also isolated and identified.

Having isolated and characterized these different phases of "GaI", we additionally wished to demonstrate their variable utility in the synthesis of low-valent gallium species. While the preparation and reactivity of low-valent gallium complexes with anionic nitrogen-based chelates have been well explored, the coordination chemistry available from phosphorus chelates is relatively unknown.[30−32] Consequently, we chose to explore the reactivity of the different "GaI" phases with the bis(phosphino)borate ligands established by Peters et al., as they have been successfully utilized in stabilizing unique low-coordinate transition-metal and main-group centers.[33−41] Using these ligands and the two distinctly different phases of "GaI", we were able to isolate complexes of Ga in all its known formal oxidation states (Ga(I), Ga(II), and Ga(III)). To the best of our knowledge, this is the first report that significantly different gallium products can be isolated from different batches of "GaI". These structures differ both from those typically formed with the anionic nitrogen chelates as well as those formed with simple neutral, monodentate phosphines, and, consequently, this report constitutes a novel expansion of the chemistry of low-valent gallium.

RESULTS AND DISCUSSION

Investigations into the Nature of "GaI". The composition of "GaI" is thought to contain a variety of gallium subiodides and also gallium metal. Information regarding structure and Raman signatures of the gallium subiodides that are of relevance to "GaI" is given below and is pertinent for the following discussion.

(1) **GaI_2**: alternatively written as Ga_2I_4, the bonding of GaI_2 is best described by the formula $[Ga^+][GaI_4^-]$. The GaI_4^- anion

dx.doi.org/10.1021/ic501139w | Inorg. Chem. 2014, 53, 9644−9656

Figure 3. Powder diffraction patterns of "GaI" as a function of reaction time: 40 min (orange) and 100 min (green). The uneven baseline is a result of the Scotch tape used to prevent exposure of the sample to air.

is in a distorted-tetrahedral geometry, with the Ga^+ cation being weakly stabilized by eight iodide atoms in the unit cell.[42] It crystallizes in the *R*3*c* space group, and its Raman spectrum features a prominent signal at 143 cm^{-1} and weaker signals at 214 and 235 cm^{-1}.[43]

(2) **Ga_2I_3**: alternatively written as Ga_4I_6, though the formula $[Ga^+]_2[Ga_2I_6^{2-}]$ is a more descriptive representation of its composition. The dianion $[Ga_2I_6^{2-}]$, with gallium in the formal Ga(II) oxidation state, possesses a Ga−Ga bond with all Ga−I bonds being terminal.[42] It crystallizes in the $P2_1/c$ space group, and its Raman spectrum features a very strong absorption at 124 cm^{-1} with weaker absorptions occurring at 292, 186, and 79 cm^{-1}.[43]

(3) **GaI_3**: structurally exists, and is sometimes written, as Ga_2I_6 with two bridging and four terminal iodine atoms and no Ga−Ga bond. The gallium atom is formally Ga(III) and is thus distinct from $[Ga_2I_6^{2-}]$. We have obtained the Raman spectrum of commercially available GaI_3 and observed very strong absorption at 142 cm^{-1} along with weaker signals at 267, 227, 194, 163, and 85 cm^{-1}.

We prepared several batches of "GaI" using Green's method of sonicating from the elements, with the reaction being stopped precisely after 40, 60, 80, and 100 min.[26] It should be noted that while the synthesis demonstrated a reasonably reliable time course, care must be taken to ensure reproducibility among reactions; changing the reaction vessel, temperature, or amount of solvent can all have dramatic influences on the rate of "GaI" conversion. The phases of "GaI" synthesized here are stable for at least 1 year at −35 °C under an inert atmosphere and showed no changes to the Raman spectra or reactivity. However, early or gray phases will begin to show a slight green color over the course of 1 week if left at room temperature under N_2. We are not certain how long this transition would require to achieve complete conversion to the exhaustively sonicated (green) phase, though the conversion may be easily identified using the techniques described below. Both phases are highly air sensitive, decomposing in minutes in an open atmosphere. Sonication for longer reaction times under the standard conditions gave a green powder with characteristics identical with those of the 100 min sample.

As the gallium subiodides have been most thoroughly characterized by Raman spectroscopy,[43−47] this was a logical entry point into the characterization of our different "GaI" samples. The synthesis of "GaI" initially yields a product with a strong absorption in the Raman spectrum at 141 cm^{-1} accompanied by weaker absorptions at 230 and 85 cm^{-1} (Figure 2). As the reaction is extended for longer times, the absorptions at 230 and 141 cm^{-1} diminish and are replaced by a strong absorption at 124 cm^{-1} and weaker absorptions at 292 and 188 cm^{-1}. There was also a corresponding color change in the produced powder from light gray to green (authentic "GaI" is generally referred to as "green"). Comparison of the vibrations observed in the Raman spectrum for the phases of "GaI" to literature values for gallium subiodides suggests that GaI_2 ($[Ga^+][GaI_4^-]$) is the dominant gallium iodide present in the early stage "GaI", while in the late-stage "GaI" Ga_2I_3 ($[Ga^+]_2[Ga_2I_6^{2-}]$) is the main gallium iodide species present.[43] The resonances observed for the "GaI" samples also strongly correlate with the Raman spectra of salts containing the relevant GaI_4^- and $Ga_2I_6^{2-}$ anions.[48−50] While some peaks for GaI_3 do overlap with those of GaI_2, the complete spectra are quite distinct and do not match either phase prepared here.

To corroborate this proposal, the powder X-ray diffraction (pXRD) patterns of our 40 and 100 min "GaI" samples were obtained. The powders do not diffract strongly; however, the observed patterns are quite distinct (Figure 3). Comparison of the pXRD patterns obtained for the two pure phases prepared by us to the literature patterns for pure GaI_2 and Ga_2I_3 indicates the expected trend; the early-phase "GaI" resembles GaI_2, while the late-phase "GaI" resembles Ga_2I_3 (Figures S-8 and S-9 in the Supporting Information).[42]

Therefore, on the basis of data obtained by Raman spectroscopy, by powder diffraction, and by application of mass and charge balance, we propose that the early-stage "GaI" sample is largely composed of $[Ga^0]_2[Ga^+][GaI_4^-]$ (simplified, $[Ga^0]_2[Ga_2I_4]$), while the late-stage "GaI" sample has the

dx.doi.org/10.1021/ic501139w | *Inorg. Chem.* 2014, 53, 9644−9656

composition $[Ga^0]_2[Ga^+]_2[Ga_2I_6^{2-}]$ (simplified, $[Ga^0]_2[Ga_4I_6]$).

We further characterized the early and late phases of "GaI" using ^{127}I nuclear quadropole resonance (NQR) spectroscopy to confirm our proposal and also identify if minor quantities of other gallium subiodides were present.[51] The frequencies of the ^{127}I NQR peaks obtained for the early-stage (40 min) and late-stage (100 min) "GaI" samples are summarized in Table 1 and the spectra are shown in Figure 4. For the early stage "GaI" sample, peaks were observed at four distinct frequencies: 113.69, 132.04, 134.39, and 163.71 MHz. These values are in excellent agreement with those obtained from the previous ^{127}I NQR study of GaI_2.[52] To verify that no GaI_3 was present, we performed ^{127}I NQR experiments at the known GaI_3 frequencies and no signal was observed.[53] For the late-stage "GaI" sample, an exhaustive search led to the observation of peaks at three distinct frequencies—106.35, 107.83, and 123.54 MHz—and no signal was obtained using the transmitter frequencies where NQR peaks were observed for either GaI_2 or GaI_3 (Figure 4). The observation of three distinct peaks is consistent with the assignment of late-stage "GaI" as Ga_2I_3, which has three crystallographically unique I atoms in its solid-state structure. The ^{127}I NQR data are therefore consistent with the previously discussed methods and also confirm that the early- and late-stage "GaI" phases contain only one gallium subiodide component.

Table 1. ^{127}I NQR Frequencies for the Early- and Late-Stage "GaI" Samples[a]

	^{127}I NQR freq (MHz)				
sample	site 1	site 2	site 3	site 4	ref
early-stage "GaI"	113.69	132.04	134.39	163.71	this study
late-stage "GaI"	106.35	107.83	123.54		this study
GaI_2	113.65	131.94	134.27	163.71	52
GaI_3	133.69	173.65	174.59		53

[a]Frequency of the $m_I = \pm 1/2 \leftrightarrow \pm 3/2$ transition at room temperature.

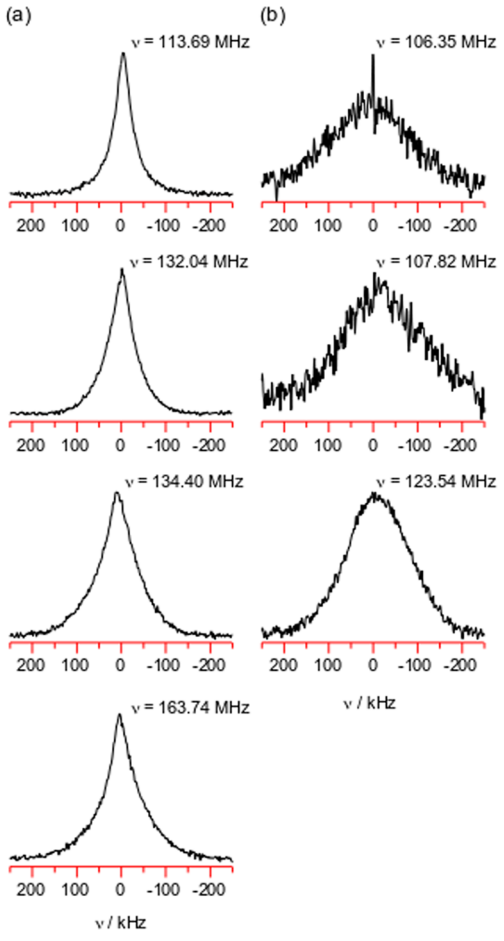

Figure 4. Experimental ^{127}I NQR spectra of (a) the four unique I sites in the early-stage "GaI" (40 min) and (b) the three unique sites in the late-stage "GaI" (100 min).

The ^{71}Ga ssNMR spectra of our "GaI" samples were obtained to provide a direct comparison to the work of Bryce and co-workers.[29] The ^{71}Ga ssNMR spectra of early-stage "GaI" (40 min), which from the above characterization methods we believe to be GaI_2, acquired at two different magnetic fields are presented in Figure 5, while the NMR spectroscopic parameters and relative amounts are summarized in Table 2. The ^{71}Ga ssNMR spectra feature a sharp, strongly deshielded peak at 4484 ppm, which has been previously assigned to Ga metal ($[Ga^0]$),[29] and a broad powder pattern centered at about −400 ppm. The ^{71}Ga powder pattern is actually a convolution of two unique powder patterns arising from two unique Ga sites within the sample: one from the $[GaI_4^-]$ component and the other from the $[Ga^+]$ component. As shown in Figure 5, each of these sites can be independently simulated and the experimental spectrum is effectively simulated by summing the two unique Ga subspectra in a 1:1 ratio. The simulation reveals that one of the Ga sites has a chemical shift of −511 ppm, a relatively small C_Q value of 1.81 MHz, and a CSA value of 85 ppm, thus giving rise to a relatively narrow powder pattern. The other site has a similar CSA value (80 ppm) but is significantly deshielded with respect to site 2 ($\delta(^{71}Ga)$ −335 ppm) and has a significantly larger C_Q value of 7.1 MHz and thus a much broader powder pattern for this site. Past liquid NMR studies have shown that the ^{71}Ga chemical shift of $[GaI_4^-]$ varies from −505 to −450 ppm.[55] Therefore, the early-stage site 1 peak, which has a shift of −511 ppm and relatively small C_Q value, can be assigned to the $[GaI_4^-]$ site within GaI_2 and the $[Ga^+]$ site assigned to the broader NMR site that has a chemical shift of −335 ppm.

The ^{71}Ga NMR spectrum of the late-stage "GaI" (100 min) sample, which we believe to contain Ga_2I_3, is presented at the bottom of Figure 6. Similar to the ^{71}Ga ssNMR spectrum of the early stage sample, there is a heavily deshielded peak at 4484 ppm, which corresponds to the $[Ga^0]$ site, and a powder pattern at about −400 ppm. The shape of the powder pattern of the late-stage sample is, however, very different from that of the early-stage sample. Even though there should be two Ga sites in Ga_2I_3—the $[Ga^+]$ site and the single Ga site in the $[Ga_2I_6^{2-}]$ dimer—the powder pattern obtained for the late-stage sample could be simulated using only one Ga site. The parameters obtained for this site are summarized in Table 2 and are similar to those previously determined for "GaI".[29]

The ^{71}Ga NMR spectra of the intermediate-stage (60 and 80 min) "GaI" samples are presented in Figure 6. Similar to the case for the early-stage and late-stage samples, the intermediate-stage samples have a strong, deshielded peak at 4484 ppm and a powder pattern centered at about −400 ppm. The powder pattern is a convolution of the GaI_2 sites and the Ga_2I_3 site, and as the reaction time increases, the relative amounts of the GaI_2 sites decrease with respect to the Ga_2I_3 site. For example, at 60 min, the ratio of GaI_2 sites 1 and 2 to Ga_2I_3 is 1:1:0.3, but at 80

dx.doi.org/10.1021/ic501139w | Inorg. Chem. 2014, 53, 9644−9656

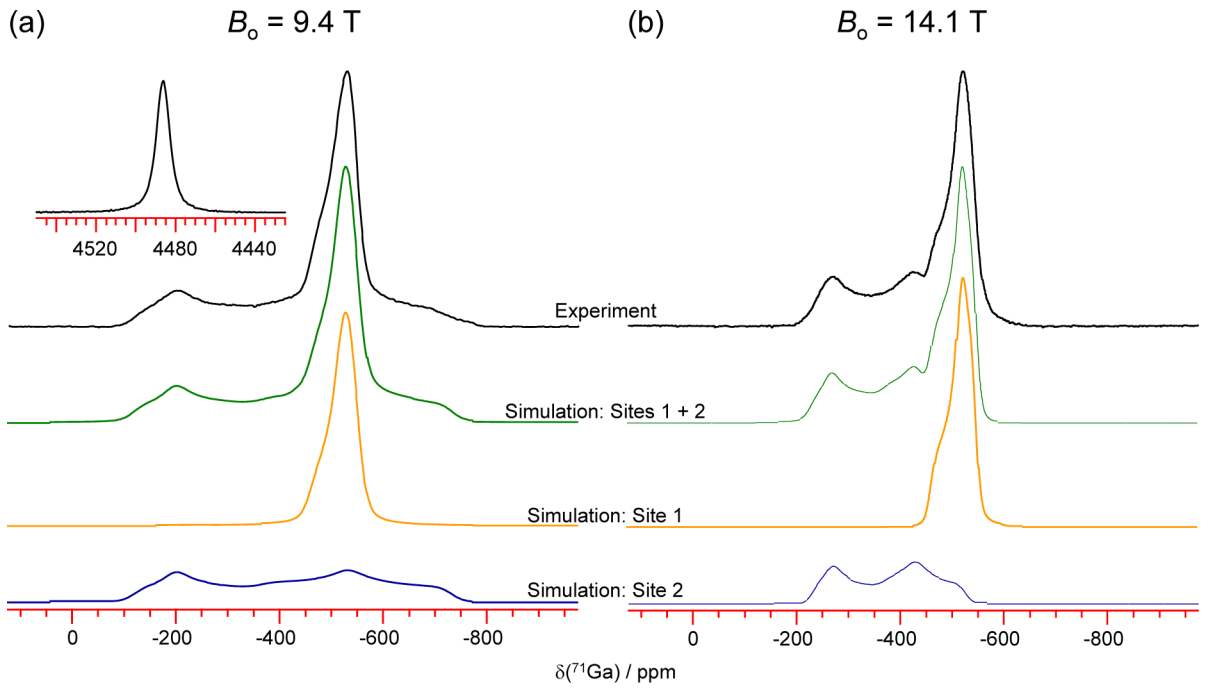

Figure 5. Experimental and simulated stationary sample solid-state ^{71}Ga NMR spectra of the early-stage "GaI" (40 min) sample, acquired at (a) B_0 = 9.04T and (b) B_0 = 14.1 T. The experimental spectrum is composed of two subspectra from the two distinct Ga sites within the sample. Each subpectrum has been simulated and then summed together in a 1:1 ratio to form the complete simulation. Inset: a strongly deshielded ^{71}Ga peak is also observed at both magnetic field strengths.

Table 2. ^{71}Ga Solid-State NMR Parameters for the Observed Ga Sites

	site				
	deshielded peak,[a] Ga^0	early stage site 1, GaI_2/ $[GaI_4^-]$	early stage site 2, GaI_2/ $[Ga^+]$	late-stage site 1, Ga_2I_3/ $[Ga^+]$	late-stage site 2,[b] Ga_2I_3/ $[Ga_2I_6^{2-}]$
			Parameters		
δ_{iso} (ppm)	4484.6(3)	−511(2)	−335(5)	−425(3)	15(5)
κ		−0.3(1)	+1	−0.07(7)	
Ω (ppm)		85(5)	80(30)	145(10)	
C_Q (MHz)		1.81(5)	7.1(3)	3.1(1)	25(1)
η_Q		1	0.38(5)	1	0.05(5)
α (deg)		0	0	41(10)	
β (deg)		70(5)	0	132(5)	
γ (deg)		0	0	24(10)	
			Ratio of Ga Sites		
reaction time					
40 min	present	1	1	0	
60 min	present	1	1	0.3(1)	
80 min	present	1	1	1.3(5)	
100 min	present	0	0	1	present

[a]Due to the large chemical shift difference between the Ga^0 peak and the remaining sites, it was difficult to determine the relative amounts of these sites with a high degree of accuracy. For example, for the late-stage (100 min) sample, depending on how the ^{71}Ga NMR spectrum was acquired, the ratio of the Ga^0 site to the Ga_2I_3 site 1 was as low as 0.25 to as high as 1.2. [b]Due to the large breadth of this site's powder pattern, we were unable to determine CSA parameters and also the amount of this site relative to those of the other sites in GaI_2 and Ga_2I_3.

min, the ratio is now 1:1:1.3. Using these ratios, the ^{71}Ga NMR spectra of the 60 and 80 min samples can be simulated. This transition from GaI_2 to Ga_2I_3 was also observed in the FT-Raman spectra of the four samples; however, the relative amounts cannot be quantified using Raman spectroscopy, while they can be using ssNMR spectroscopy.

As mentioned above, it was surprising that for the late-stage "GaI" sample, which has been shown to possess Ga_2I_3, only one Ga site was observed even though there are two distinct Ga sites in Ga_2I_3.[42] A closer examination of the ^{71}Ga ssNMR spectrum of Ga_2I_3 revealed several small bumps in the baseline, which we originally assumed were simply artifacts. To be certain, the ^{71}Ga ssNMR spectrum of Ga_2I_3 was reacquired using a quadrupolar Carr−Purcell−Meiboom−Gill (QCPMG)[56] experiment combined with WURST pulses.[57] Using these approaches, we were able to obtain the ^{71}Ga NMR spectrum of the second Ga site within Ga_2I_3 (Figure 7). The powder pattern for this site is extremely broad, over 700 kHz at

dx.doi.org/10.1021/ic501139w | Inorg. Chem. 2014, 53, 9644−9656

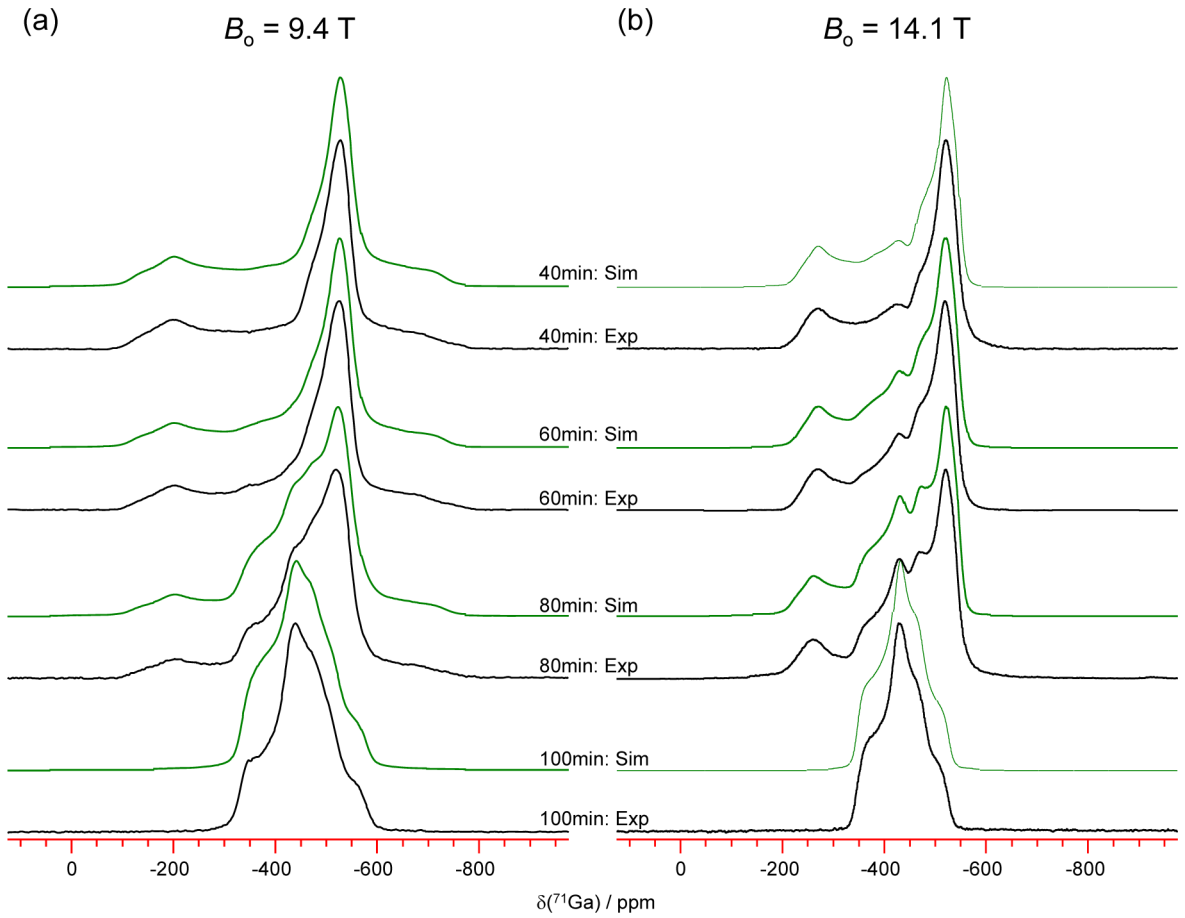

Figure 6. Experimental and simulated stationary sample solid-state ^{71}Ga NMR spectra of the "GaI" early-stage (40 min), intermediate-stage (60 and 80 min), and late-stage (100 min) samples acquired at (a) B_0 = 9.04 T and (b) B_0 = 14.1 T. The displayed region of the spectrum of the early-stage sample was simulated using two distinct Ga sites that correspond to the $[Ga^+]$ and $[GaI_4^-]$ environments in GaI_2. In the displayed region of the late-stage sample, which we know to be Ga_2I_3, only one of its $[Ga^+]$ and $[Ga_2I_6^{2-}]$ Ga sites give rise to an observable NMR signal. The simulated spectra of the intermediate-stage samples are convolutions of the spectra of GaI_2 and Ga_2I_3, where the relative amount of GaI_2 decreases with respect to that of Ga_2I_3 as the reaction time increases.

B_0 = 9.4 T, in comparison to the other Ga site in Ga_2I_3 and either Ga site in GaI_2. The ^{71}Ga C_Q value of this second Ga_2I_3 site is 25 MHz, while for the first site the C_Q value was only 3.1 MHz. The massive difference in the breadths of the two powder patterns has two consequences. The first is that the intensity of site 2 is very weak in comparison to that of the much narrower site 1, and as a result the signal from site 2 was simply lost in the baseline of the spin−echo NMR spectra. The second is that it is not possible to accurately determine the relative amounts of the two Ga sites present in the late-stage "GaI" sample.

In addition to having a significant difference in C_Q values, the chemical shifts also differ significantly between the two sites: −425 ppm for the first site, in comparison to +15 ppm for the second site. Thus, the first site in Ga_2I_3 has a C_Q value and chemical shift that are comparable to the values for the two sites found in GaI_2, whereas the second site in Ga_2I_3 has significantly different C_Q and chemical shift values. From this, a tentative assignment of the NMR sites to the two Ga sites in Ga_2I_3 can be made. In Ga_2I_3, there is a $[Ga^+]$ similar to that found in GaI_2, plus a $[Ga_2I_6^{2-}]$ dimer that is unique to Ga_2I_3. It would be expected that the NMR spectroscopic parameters for the $[Ga^+]$ site in Ga_2I_3 would be similar to those observed for the $[Ga^+]$ site in GaI_2. From this, we assign the first NMR site in Ga_2I_3 to $[Ga^+]$. The second NMR site in Ga_2I_3 is thus the $[Ga_2I_6^{2-}]$ dimer, where each Ga in the dimer sits in the center of a distorted I_3−Ga−Ga tetrahedron. Of the two "GaI" samples, this is the only Ga site where the nearest neighbor atoms are not all I. When GaI_4^- is considered, it is well-known that as the I atoms are replaced by other atoms the ^{71}Ga chemical shift becomes more deshielded.[58] For example, the ^{71}Ga chemical shift of $[GaI_4^-]$ in CH_2Cl_2 is −455 ppm and increases to −310 ppm for $[GaBrI_3^-]$ and to −235 ppm for $[GaClI_3^-]$.[59] Therefore, it is not surprising that the $[Ga_2I_6^{2-}]$ dimer site in Ga_2I_3 has a unique chemical shift value in comparison to the other Ga sites in Ga_2I_3 and GaI_2.

There exists a curious disagreement between the ^{127}I NQR data and ^{71}Ga solid-state NMR data acquired in our study versus those acquired in the study by Bryce and co-workers.[29] The ^{71}Ga solid-state NMR parameters for our late-stage "GaI", which we have assigned to Ga_2I_3, match the ^{71}Ga ssNMR parameters determined by Bryce and co-workers for their "GaI" sample. However, for their "GaI" sample, they reported ^{127}I NQR frequencies of 113.69, 132.03, and 134.375 MHz and thus assigned their compound to be GaI_2 (or more formally $[Ga^0]_2[Ga]^+[GaI_4]^-$).[29] For our late-stage "GaI" sample, no ^{127}I NQR signals were obtained at those frequencies. These known ^{127}I NQR frequencies for GaI_2 were present in our early-stage "GaI", although the solid-state ^{71}Ga ssNMR parameters for that "GaI" sample do not match those determined by Bryce and co-

dx.doi.org/10.1021/ic501139w | Inorg. Chem. 2014, 53, 9644−9656

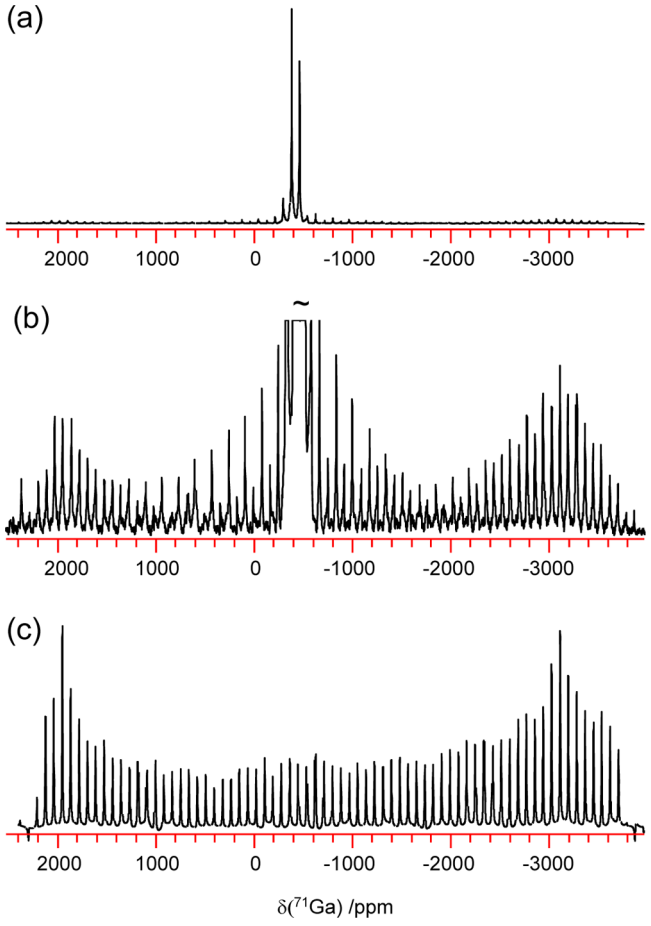

Figure 7. Experimental and simulated stationary sample solid-state WURST QCPMG ^{71}Ga NMR spectra of late-stage (100 min) "GaI" acquired at B_0 = 9.04 T: (a) experimental spectrum, with the vertical scale normalized to the height of the site 1 peaks; (b) spectrum with the vertical scale increased to emphasize the second, broader Ga site; (c) simulated spectrum of the second Ga site.

workers. We do not propose an explanation for this discrepancy, although we do note that, when performing the ^{127}I NQR, we performed ^{71}Ga ssNMR both before the NQR experiments and after the NQR experiments to verify the composition of the sample.

In summary, the results obtained from Raman spectroscopy, I^{127} NQR spectroscopy, ^{71}Ga ssNMR spectroscopy, and pXRD are self-consistent and indicate that the initial phase of "GaI" obtained in Green's synthesis is $[Ga^0]_2[Ga^+][GaI_4^-]$, while the late phase of "GaI" is $[Ga^0]_2[Ga^+]_2[Ga_2I_6^{2-}]$. These reagents are controllably synthesized and can be stored for long periods of time, and their identity is quickly confirmed using common solid-state techniques.

Reactions of Bis(phosphino)borate Ligands with "GaI". Having obtained and characterized "GaI" phases of differing structural composition, we wished to determine whether or not each phase possessed a unique reactivity. Consequently, we attempted the 1:2 stoichiometric reaction of $Tl[Ph_2B(CH_2PPh_2)_2]$ (**1**)[33] with early "GaI" in both THF and benzene solutions (Scheme 1). Upon mixing the rapid precipitation of an orange powder was observed, consistent with the elimination of TlI. Phosphorus-31 NMR spectroscopy of the reaction mixture showed a dramatic transition from a broad doublet that characterizes the free ligand (δ_P 52.6, $^1J_{Tl-P}$ = 4166 Hz) to several sharp resonances below δ_P 0, with the most significant occurring as a singlet (δ_P −1.8 in THF). Structural characterization of this product was achieved from X-ray diffraction analysis of single crystals grown by vapor diffusion of pentane into a THF solution of the purified powder. Modeling of the X-ray data indicates that the product is a Ga(II) dimer featuring a formally dicationic Ga_2I_2 fragment (**3**).

The reaction was then repeated, varying only the batch of "GaI" that was employed. Monitoring the resulting reaction mixtures by $^{31}P\{^1H\}$ NMR spectroscopy (Figure 8, left) demonstrated that each "GaI" unique combination of early and late "GaI" phases produced different mixtures of products. Aside from **3**, these products proved difficult to isolate, and to date we have not been able to isolate and characterize any other species in these reaction mixtures. Therefore, it was decided to employ a related bis(phosphino)borate, $[Li(THF)_2(P^iPr_2CH_2)_2BPh_2]$ (**2**),[33] in the hope of obtaining more tractable product mixtures (Scheme 1). The reaction of **2** with the different batches of "GaI" in THF gave a new set of unique product mixtures (Figure 8, right). X-ray-quality crystals grown from the reaction with early "GaI" yielded the solid-state structure of **4** (δ_P 15 in THF), the structural analog of **3**, though we were unable to isolate this product cleanly in bulk. An additional product, as determined by $^{31}P\{^1H\}$ NMR spectroscopy (δ_P 14 in THF), was isolated as a white powder from the reaction mixture involving the late "GaI" (100 min). The ^{1}H NMR data revealed an asymmetric ligand environment and a substantial amount of THF, even after prolonged drying. Single crystals of this product that were suitable for X-ray diffraction were grown by vapor diffusion of pentane into a THF solution of the purified powder. Analysis of the resulting X-ray diffraction data revealed the product to be **5** (Scheme 1), a lithium−THF salt involving a $\{Ga_2I_4\}$ bis(phosphino)borate

Scheme 1. Synthesis of Dimeric (3, 4) Ga_2I_2 Gallium−Phosphorus Coordination Compounds and the Unusual Base-Stabilized Ga_2I_4 Fragment (5) Isolated from the Reaction of Bis(phosphino)borate Ligands (1, 2) with Different "GaI" Samples

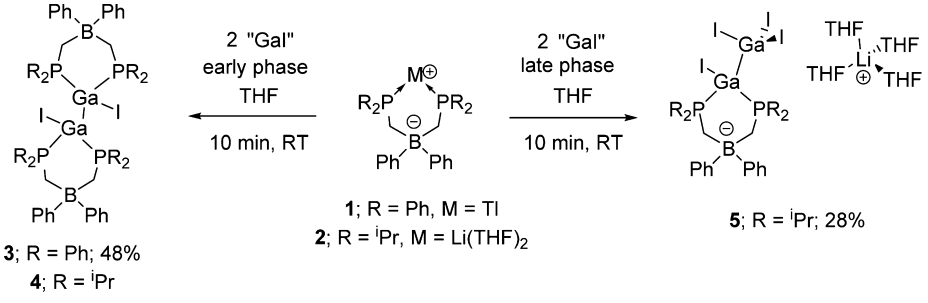

3; R = Ph; 48%
4; R = ^{i}Pr

1; R = Ph, M = Tl
2; R = ^{i}Pr, M = Li(THF)$_2$

5; R = ^{i}Pr; 28%

dx.doi.org/10.1021/ic501139w | Inorg. Chem. 2014, 53, 9644−9656

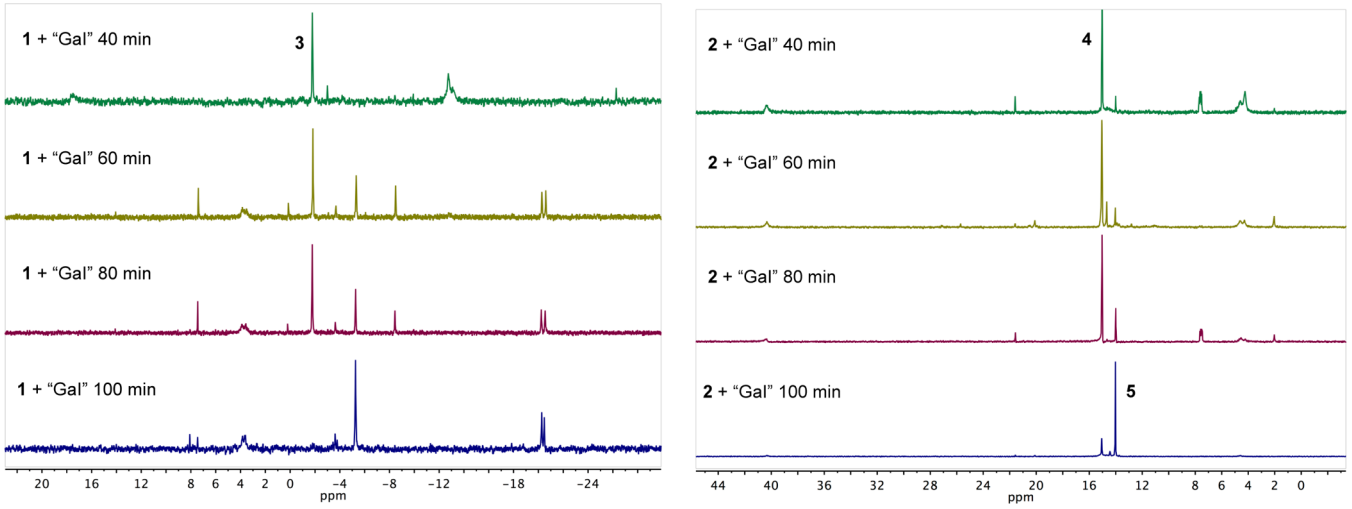

Figure 8. Effect of the type of "GaI" on the outcome of the reaction with the bis(phosphino)borate ligands **1** (left) and **2** (right). A stack plot of ^{31}P NMR spectra is shown, highlighting the range of products observed. Total reaction times for the preparation of the "GaI" used in each reaction are noted adjacent to the relevant spectrum.

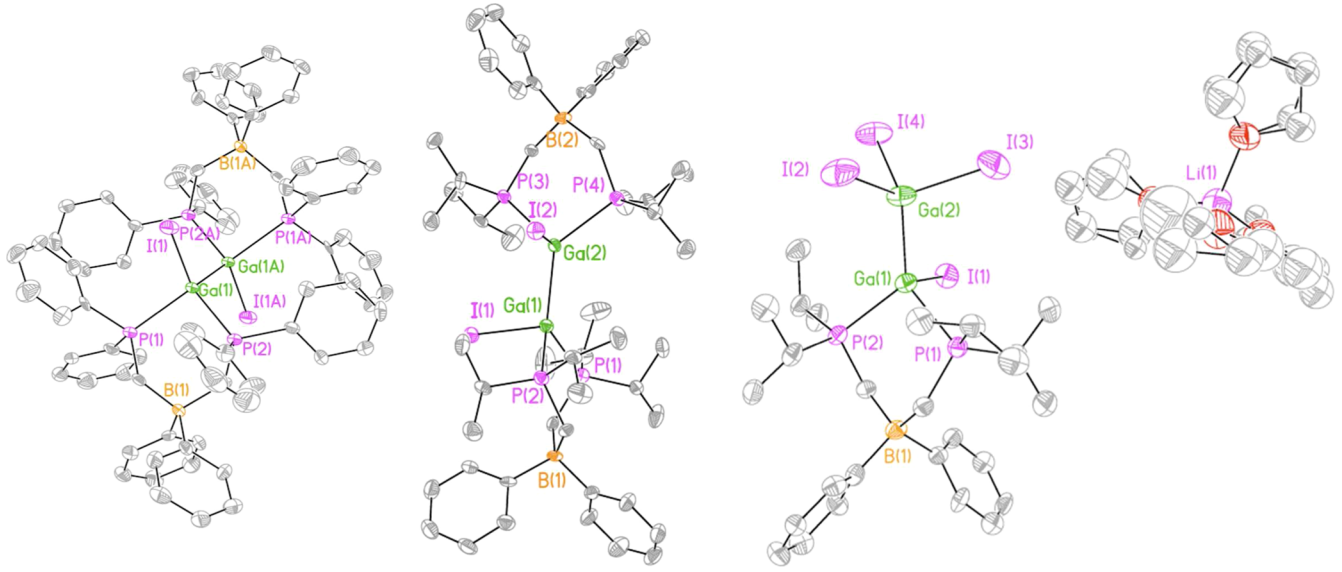

Figure 9. Solid-state structures of the feature compounds **3**−**5** (from left to right, respectively). Ellipsoids are drawn at the 50% probability level, and hydrogen atoms are removed for clarity. Selected metrical parameters are given in Table 4, while crystallographic details are given in Table 5

anion. In contrast to the reactions with the thallium bis(phosphino)borate **1**, salt elimination does not occur and the charge of the anionic gallium complex is balanced by a lithium cation that possesses four THF molecules in its coordination sphere.

To determine if the variable reactivity of the different "GaI" phases would continue to hold across a range of reactions, we chose to attempt the reaction of different "GaI" samples with the β-diketiminate ligand Li{(NDippCMe)$_2$CH (**6**; Dipp = C$_6$H$_3$^{i}Pr$_2$-2,6), to yield N-heterocyclic gallium species previously reported by Power et al.[6] By treating **6** with 1.5 stoichiometric equivalents of "GaI" in benzene and stirring for 1 h, crude mixtures whose contents could be analyzed by ^{1}H NMR spectroscopy were obtained. Signals that are diagnostic of Ga(I) and Ga(III) products for Ga{(NDippCMe)$_2$CH} (**7**) and I$_2$Ga{(NDippCMe)$_2$CH} (**8**), respectively, in addition to some protonated ligand were observed (Figures S-34−S-40, Supporting Information). For the early-phase "GaI" a fourth set of peaks consistent with a related complex are also observed. We hypothesize that this compound may be indicative of a Ga(II) product, though we were unable to isolate and characterize such a species (N-heterocyclic Ga(II) compounds have precedent in the literature).[5,60] This would be consistent with our observation that Ga(II) products are produced from the early-phase "GaI" as well as literature reports of the formation of Ga(II) products from the reaction between GaI$_2$ and simple donor ligands,[61−63] despite the formal Ga(I) and Ga(III) centers in the crystal structure.[64] The increased ratio of Ga(I) product for the late-phase "GaI" in comparison to the early-phase "GaI" is potentially a result of the larger mole percent of Ga$^+$ ions in the overall formula: 8.9% Ga$^+$ in the early phase "GaI" ([Ga^0]$_2$[Ga$^+$][GaI$_4^-$]) and 11.8% Ga$^+$ in the late-phase "GaI" ([Ga^0]$_2$[Ga$^+$]$_2$[Ga$_2$I$_6^{2-}$]). Obviously the structure−reactivity relationship is affected by complex redox and disproportionation reactions that are still not understood. However, it is hoped that the correct assignment of the

dx.doi.org/10.1021/ic501139w | Inorg. Chem. 2014, 53, 9644−9656

structure of different phases of "GaI" will provide some measure of control in the synthesis of new low-valent gallium compounds.

X-ray Crystallography. The solid-state structures of **3**–**5** are shown in Figure 9, while the X-ray parameters and relevant bond distances and angles are given in Tables 4 and 5, respectively. The monomeric form of compound **3** sits on an inversion center. The Ga–Ga bond length is 2.4666(17) Å, while the Ga–I bond length is 2.5755(14) Å. The Ga–P bond lengths are slightly different at 2.401(2) and 2.448(2) Å and are long in comparison to traditional Ga–P covalent bonds (cf. 2.31–2.37 Å)[60,65,66] and comparable to those in compounds that can be described as donor→acceptor complexes (cf. 2.40–2.48 Å).[30,32,67] The P–Ga–P bond angle is fairly small at 92.98(7)°, while the I–Ga–Ga–I torsion angle is 0° due to the symmetry of the molecule. This structure may be compared to a related Ga(II) dimer isolated by Schnöckel et al. which consists of a $\{Ga_2I_4\}$ fragment stabilized by two $P(CH_2CH_3)_3$ molecules.[31] The Ga–Ga, Ga–P, and Ga–I bond lengths are all quite similar at 2.436(2), 2.414(3), and 2.58–2.59(1) Å, respectively. Compound **4**, $[(\mathbf{2})Ga_2I_2(\mathbf{2})]$, has the same phosphine-stabilized $[Ga_2I_2]^{2+}$ core seen in **3**; however, **4** adopts a different structural conformation than **3** with the I–Ga–Ga–I torsion angle being 97.85(2)° instead of perfectly linear. As a result, the bis(phosphino)borate ligands are twisted relative to each other, highlighting the unique structural changes that can be observed by varying the substituents on phosphorus. The Ga–Ga bond length and two Ga–I bond lengths are 2.4999(7), 2.6257(6), and 2.6367(6) Å, respectively. The Ga–P bond lengths are again consistent with dative bonds at 2.4239(14), 2.4439(13), 2.4246(13), and 2.4529(13) Å. The P–Ga–P bond angles are somewhat different at 95.29(5) and 99.34(4)°, a likely result of the flexibility of the ligand framework. For compound **5**, $[Li(THF)_4]^+[(\mathbf{2})GaIGaI_3]^-$, the Ga–Ga and two Ga–P bond lengths are 2.4521(11), 2.3906(15), and 2.4027(16) Å, respectively. The

Table 4. Significant Metrical Parameters for 3–5[a]

	3	4	5
Ga–P	2.401(2)	2.4239(14)	2.3906(15)
	2.448(2)	2.4439(13)	2.4027(16)
		2.4246(13)	
		2.4529(13)	
Ga–Ga	2.4666(17)	2.4999(7)	2.4521(11)
Ga–I	2.5755(14)	2.6257(6)	2.6167(14)
		2.6367(6)	2.6055(14)
			2.6082(11)
			2.6181(11)
P–Ga–P	92.98(7)	95.29(5)	96.92(5)
		99.34(4)	
I–Ga–Ga–I	0	97.85(2)	

[a]Bond lengths are given in Å and bond angles in deg.

Table 5. X-ray Details for 3–5

	3	4	5
formula	$C_{76}H_{68}B_2Ga_2I_2P_4$	$C_{67}H_{99}B_2Ga_2I_2P_4$	$C_{42}H_{74}BGa_2I_4LiO_4P_2$
formula wt	1520.1	1443.27	1369.74
crystal dimens, mm	0.065 × 0.080 × 0.110	0.034 × 0.47 × 0.121	0.100 × 0.120 × 0.302
crystal color and habit	colorless prism	colorless needle	colorless needle
crystal syst	triclinic	monoclinic	triclinic
space group	$P\bar{1}$	$P2_1/n$	$P\bar{1}$
temp, K	150	150	150
a, Å	12.644(3)	10.4865(9)	11.109(2)
b, Å	13.368(3)	29.148(2)	15.256(3)
c, Å	13.342(3)	22.9354(18)	17.476 (4)
α, deg	106.16(3)	90	105.18(3)
β, deg	93.01(3)	100.284(2)	93.18(3)
γ, deg	110.49(3)	90	104.20(3)
V, Å^3	2014.1(7)	6897.7(10)	2748.2(10)
Z	1	4	2
F(000)	762	2956	1340
ρ, g/cm	1.253	1.390	1.655
λ(Mo K*α*), Å	0.71073	0.71073	0.71073
μ, cm^{-1}	1.551	1.806	3.319
max 2*θ* for data collection, deg	50.70	51.42	55.84
measd fraction of data	0.977	0.993	0.976
no. of rflns measd	22320	60725	23164
no. of rflns measd	7200	13067	12856
R_{merge}	0.0835	0.1278	0.0445
no. of rflns included in refinement	7200	13067	12856
no. of params in least squares	388	710	635
R1, wR2[a]	0.0626, 0.1401	0.390, 0.0421	0.0491, 0.1091
R1, wR$_2$ (all data)[a]	0.1124, 0.1530	0.1175, 0.0505	0.1107, 0.1313
GOF[a]	0.980	0.706	1.038
min, max peak heights on final Δ*F* map, e/Å	1.796, −1.312	0.578, −0.600	1.620, −1.760

[a]R1 = $\sum(|F_o| - |F_c|)/\sum F_o$. wR2 = $[\sum(w(F_o^2 - F_c^2)^2)/\sum(wF_o^4)\ ]^{1/2}$. GOF = $[\sum(w(F_o^2 - F_c^2)^2)/((\text{no. of rflns}) - (\text{no. of params}))]^{1/2}$.

dx.doi.org/10.1021/ic501139w | Inorg. Chem. 2014, 53, 9644–9656

Ga−P bond lengths in **5** are nearly identical, and the average distance is slightly less than that observed in **3**. The Ga−I bond distance for the {GaI} fragment is 2.6167(14) Å, while those for the $\{GaI_3\}$ fragment are 2.6055(14), 2.6082(11), and 2.6181(11) Å. All four of these bond lengths are longer than the Ga−I distance observed in **3**. The P−Ga−P bond angle is 96.92(5)°, while the P−Ga−I bond angles are significantly smaller (cf. 100−101°) than the P−Ga−Ga bond angles (cf. 121−126°). The Li−O bond lengths for the $Li(THF)_4$ cation are reasonably consistent, considering the inherent disorder of the THF molecules and range from 1.90 to 1.94 Å. The gallium atoms in both **3** and **4** are in a distorted-tetrahedral geometry, consistent with being four-coordinate and electronically satisfied.

CONCLUSIONS

By examining the composition of different "GaI" samples, prepared by varying the sonication time, convincing new structural insights regarding the appropriate assignment of "GaI" were obtained. It was demonstrated through comprehensive solid-state characterization methods that GaI_2 is the first gallium subiodide phase produced when using Green's method of sonication of the elements, followed by quantitative conversion to Ga_2I_3 over the course of the reaction. Gallium metal is present in both phases to give an overall structural composition of $[Ga^0]_2[Ga^+][GaI_4^-]$ (simplified, $[Ga^0]_2[Ga_2I_4]$) for the early-stage "GaI" and $[Ga^0]_2[Ga^+]_2[Ga_2I_6^{2-}]$ (simplified, $[Ga^0]_2[Ga_4I_6]$) for the late-stage "GaI". The intermediate phases contain a mixture of both extremes with no other observable gallium iodine compounds (i.e. GaI_3). These phases are easily and reproducibly prepared by controlling the reaction time, while the samples may be routinely analyzed by FT-Raman spectroscopy and powder X-ray diffraction. In addition, ssNMR and NQR spectroscopy may also be used to quickly characterize, and identify, the "GaI" phase present after synthesis. Gallium chemists can now use widely accessible techniques to provide diagnostic information on the "GaI" they have prepared and potentially gain a handle on the reactivity it may exhibit. This is significant, as it was further demonstrated that each unique composition possesses a unique reactivity through the synthesis of gallium−phosphorus coordination compounds. The zwitterionic Ga(II) dimers **3** and **4** feature a formal "$Ga_2I_2^{2+}$" core stabilized by the anionic bis(phosphino)-borate ligands, while the product **5** may be thought of as a Lewis acid−base adduct between a bis(phosphino)borate-stabilized {GaI} fragment and GaI_3. The synthetic results underscore the importance of identifying the nature of the "GaI" prepared to obtain consistent reactivity.

EXPERIMENTAL SECTION

General Procedures. All inert atmosphere syntheses were performed in a nitrogen-filled MBraun Labmaster 130 glovebox or using standard Schlenk-line techniques unless otherwise stated. The bis(phosphino)borates were prepared from the materials described below by the literature procedures.[33] Phenylmagnesium bromide (1 M in THF), boron trichloride (1 M in heptane), methyllithium (1.6 M in Et_2O), chlorodiphenylphosphine, *n*-butyllithium (2 M in cyclohexane), and diisopropylchlorophosphine were obtained from Sigma-Aldrich. Dimethyltin dichloride, thallium(I) nitrate, and dimethyldiphenyltin were obtained from Alfa Aesar. *N*,*N*,*N*′,*N*′-Tetramethylethylenediamine (TMEDA, obtained from Alfa Aesar) was stirred over NaOH, distilled under vacuum, and stored in a Strauss flask under N_2. All other reagents were used as received. Both elemental gallium and iodine were obtained from Sigma-Aldrich. Solvents were obtained from Caledon Laboratories and dried and deoxygenated in an MBraun Atmosphere Controlled Solvent Purification System. Dried solvents were collected under vacuum and stored as follows. Acetonitrile was stored under a nitrogen atmosphere in Strauss flasks or in the glovebox over 3 Å molecular sieves. All other solvents were stored under a nitrogen atmosphere in Strauss flasks or in the glovebox over 4 Å molecular sieves. All solvents used in NMR spectroscopy were obtained from Cambridge Isotope Laboratories and dried with CaH_2, distilled under vacuum, and stored in the glovebox over 4 Å molecular sieves. Solution ^1H, $^{13}C\{^1H\}$, $^{11}B\{^1H\}$, and $^{31}P\{^1H\}$ NMR spectra were recorded on a Varian INOVA 400 MHz or a Varian INOVA 600 MHz spectrometer as noted (for the 400 MHz spectrometer, ^1H 400.09 MHz, $^{11}B\{^1H\}$128.23 MHz, $^{13}C\{^1H\}$ 100.52 MHz, $^{31}P\{^1H\}$ 161.82 MHz; for the 600 MHz spectrometer, ^1H 599.5 MHz $^{13}C\{^1H\}$ 150.78 MHz, $^{31}P\{^1H\}$ 242.89 MHz). All ^1H and ^{13}C NMR samples were referenced to the solvent signal relative to $Si(CH_3)_4$ ($CDCl_3$, ^1H δ_H 7.26, ^{13}C δ_C 77.16; C_6D_6, ^1H δ_H 7.16, $^{13}C\{^1H\}$ δ_C 128.06; CD_3CN, ^1H δ_H 1.95, $^{13}C\{^1H\}$ δ_C 1.32, 118.26). Chemical shifts for $^{31}P\{^1H\}$ and $^{11}B\{^1H\}$ NMR spectroscopy were referenced to an external standard (85% H_3PO_4, δ_P 0 ppm; $BF_3(Et_2O)$, δ_B 0 ppm). Fourier transform infrared spectroscopy was performed on samples as KBr pellets using a Bruker Tenser 27 FT-IR spectrometer with a resolution of 4 cm^{-1}. Fourier transform Raman spectroscopy was performed on samples that were flame-sealed in glass capillaries using a Bruker RFS 100/S spectrometer, with a resolution of 4 cm^{-1}. Mass spectrometry was recorded in house in positive and negative ion modes using an electrospray ionization Micromass LCT spectrometer. Melting or decomposition points were determined by flame-sealing the sample in capillaries and heating using a Gallenkamp Variable Heater. The "GaI" was prepared in a Elma E 60 H Elmasonic ultrasonic bath set to 30 °C.

Single-Crystal X-ray Crystallography. The single-crystal X-ray diffraction studies were performed at the Western University X-ray facility. Crystals were selected under Paratone(N) oil, mounted on a Mitegen polyimide micromount, and immediately put under a cold stream of nitrogen for data to be collected on a Nonius Kappa-CCD area detector or Bruker Apex II detector using Mo Kα radiation (λ = 0.71073 Å). The Nonius and Bruker instruments operate SMART[68] and COLLECT[69] software, respectively. The unit cell dimensions were determined from a symmetry -constrained fit on the full data set, which was composed of φ and ω scans. The frame integration was performed by SAINT,[70] the resulting raw data were scaled, and absorption was corrected using a multiscan averaging of symmetry-equivalent data using SADABS.[71] The SHELXTL/PC V6.14 for Windows NT suite of programs was used to solve the structure by direct methods.[72] Subsequent difference Fourier syntheses allowed the remaining atoms to be located, while hydrogen atoms were placed in the calculated positions and allowed to ride on the parent atom. In all cases the gallium bis(phosphino)borate components were well ordered and refined with anisotropic thermal parameters. The $Li(THF)_4$ cation in **4** possesses three disordered solvate molecules that can each be refined over two positions, while the fourth THF solvate is partially disordered. The model refines satisfactorily, with all carbon atoms being refined anisotropically. The thermal parameters were restrained with SIMU and DELU commands. The related C−C and C−O bond lengths in these disordered molecules were restrained to be identical by using the SAME command. Certain C−C and C−O bond lengths were restrained to sensible values with the aid of the DFIX command. Two disordered solvents (THF and CH_2Cl_2) were present in the unit cell of **3**. We were unable to model the solvent molecules, even with the use of restraints, and thus their electron density was treated as a diffuse contribution to the overall scattering by Squeeze/Platon (total 129 electrons).

Powder Diffraction. The powder diffraction studies were performed on an Inel CPS Powder diffractometer using Cu Kα radiation from an Inel XRG 3000 generator and a CPS 120 detector. The samples were ground to a fine powder with a mortar and pestle and sealed on an aluminum dish with Scotch tape (Scotch 3M Magic Tape 810D). After 90 min the signals attributable to "GaI" and the Scotch tape (broad signal between 5 and 20° 2θ) were clearly observed. These data were processed using the ACQ software and

dx.doi.org/10.1021/ic501139w | Inorg. Chem. 2014, 53, 9644−9656

compared to literature patterns using the Match software. The powder patterns for GaI_2 and Ga_2I_3 are accessible from the PDF-4+ database with the numbers 04-007-1340 and 04-007-1339, respectively. It should be noted that no suitable diffraction pattern is observed if the samples are packed in a flame-sealed capillary.

Solid-State NMR Spectroscopy. Solid-state ^{71}Ga NMR experiments were performed using a Varian Infinity Plus 400 NMR spectrometer ($\nu_L(^{71}Ga)$ = 121.78 MHz) equipped with a Varian 5 mm quadrupole-resonance HFXY magic-angle spinning NMR probe and a Varian Inova 600 NMR spectrometer ($\nu_L(^{71}Ga)$ = 182.67 MHz) equipped with a Varian 3.2 mm triple-resonance HXY magic-angle spinning probe. The powder samples were stored inside a nitrogen-gas glovebox filled with nitrogen gas and packed tightly into either 5 or 3.2 mm o.d. ZrO_2 rotors and then sealed. At both magnetic field strengths, the FIDs were acquired using either a $\pi/2-\tau_1-\pi/2-\tau_2-$acq or a $\pi/2-\tau_1-\pi-\tau_2-$acq spin−echo pulse sequence, where $\tau_2 < \tau_1$, and the spectra were referenced with respect to the ^{71}Ga peak of a 1.0 M aqueous $Ga(NO_3)_3$ solution ($\delta(^{71}Ga)$ 0.0 ppm). On the 400 MHz spectrometer, 4096 scans were summed using a selective 1.7 μs $\pi/2$-pulse width, 800 kHz spectral width, 30 μs τ_1, 1 s recycle delay, and 12.8 ms acquisition time. On the 600 MHz spectrometer, between 3104 and 16000 scans were summed using a selective 0.25 μs $\pi/2$-pulse width, 500 kHz spectral width, 30 μs τ_1, 1 s recycle delay, and 4.1 ms acquisition time. For processing, the FIDs were left-shifted to the top of the half-echo; 1 zero-fill and 400 Hz of line broadening were applied before Fourier transform.

To observe the broad site in the 100 min sample, stationary-sample ^{71}Ga quadrupolar Carr−Purcell−Meiboom−Gill (QCPMG)[56] spectra were acquired on both the Infinity Plus 400 and Inova 600 NMR spectrometers. On the latter instrument, a total of 13 individual spectra were acquired, where the transmitter frequency varied by 50 kHz between each spectrum, and summed together to generate the entire powder pattern. Each individual spectrum was acquired using 1024 scans, a 4.0 μs $\pi/2$-pulse width, 500 kHz spectral width, 1 s recycle delay, 4.96 ms total acquisition time, and an echo train consisting of 48 π-pulses. The interpulse delays were set in order to achieve a 10 kHz spacing between the individual spikelets. On the former instrument, the WURST-QCPMG[57] variant was utilized and thus the powder pattern could be fully excited in one experiment. The spectrum was acquired using 12600 scans, 10 μs WURST pulses, 700 kHz offset, 2500 kHz spectral width, 1 s recycle delay, 5.39 ms total acquisition time, and an echo train consisting of 55 WURST pulses. The interpulse delays were set in order to achieve a 10 kHz spacing between the individual spikelets.

Stationary-sample ^{71}Ga NMR spectra are broadened by the quadrupolar interaction between the nuclear quadrupole moment of ^{71}Ga and the molecule's electric field gradient (EFG), plus the orientation dependence of the chemical shift (chemical shift anisotropy, CSA). The EFG and CSA are both second-rank interaction tensors that in their principal axis system can be described by three principal components. The EFG tensor is represented by V_{XX}, V_{YY}, and V_{ZZ}, where $|V_{XX}| \leq |V_{YY}| \leq |V_{ZZ}|$, and the CS tensor can be represented by δ_{11}, δ_{22}, and δ_{33}, where $\delta_{11} \geq \delta_{22} \geq \delta_{33}$. Simulations of the experimental NMR spectra were performed using the WSolids1 software developed by Klaus Eichele[73] and require parameters describing the quadrupolar interaction, the CS tensor, and Euler angles that describe the relative orientation of the EFG and CS tensors.[74−76] The quadrupolar interaction is described by two parameters: the quadrupolar coupling constant $C_Q = eQV_{33}h^{-1}$, where e is the elementary charge, Q is the ^{71}Ga nuclear quadrupole moment, and h is Planck's constant, and the asymmetry parameter $\eta_Q = (V_{XX} - V_{YY})/V_{ZZ}$. The chemical shift tensor is described by three parameters: the isotropic chemical shift $\delta_{iso} = (\delta_{11} \geq \delta_{22} \geq \delta_{33})/3$, the span $\Omega = \delta_{11} - \delta_{33}$, and the skew $\kappa = 3(\delta_{22} - \delta_{iso})\Omega^{-1}$.[79] The relative orientations of the EFG and CS tensors are described by three Euler angles: α, β, and γ. Different conventions for the Euler angles exist, and we utilized the ZYZ convention as implemented in the WSolids1 software.

Nuclear Quadrupole Resonance. ^{127}I nuclear quadrupole resonance experiments were performed on the 40 and 100 min "GaI" samples using a Varian Inova 600 NMR spectrometer equipped with a Varian 4 mm triple-resonance HXY magic-angle spinning NMR probe. The samples were packed tightly into 4 mm o.d. ZrO_2 rotors inside a nitrogen-filled glovebox and then sealed before being transferred to the probe. The probe was placed roughly 3 m from the edge of the NMR magnet and was purged continuously with nitrogen gas. For the 40 min sample, the spectra were acquired using a $\pi/2-\tau_1-\pi-\tau_2-$acq spin−echo pulse sequence, where τ_1 was 30 μs and τ_2 was 15 μs. A total of 2048 scans were summed using a 1.05 μs $\pi/2$-pulse width, 500 kHz spectral width, 0.5 s recycle delay, and 256 μs acquisition time. The transmitter frequencies attempted included the known ^{127}I NQR frequencies for GaI_3[58] ($\nu(m_I = \pm1/2 \leftrightarrow \pm3/2)$ = 133.69, 173.65, and 174.59 MHz) and for GaI_2 ($\nu(m_I = \pm1/2 \leftrightarrow \pm3/2)$ = 113.65, 131.94, 134.27, and 163.71 MHz). For processing, the FIDs were left-shifted to the top of the half-echo; 1 zero-fill and 500 Hz of line broadening were applied before Fourier transform. For the 100 min sample, experiments were performed and processed in the same manner as for the 40 min sample, except the transmitter frequency was varied from 176.6 to 104.0 MHz in 0.2 MHz increments and 256 scans were summed. Once an NQR frequency was observed, the transmitter was placed "on-resonance" and 2048 scans were summed.

Literature Procedures. $Tl[Ph_2B(CH_2PPh_2)_2]$ (**1**) and $[Li(THF)_2(P^iPr_2CH_2)_2BPh_2]$ (**2**) were prepared according to the procedure of Peters,[33] with the exception that a solution of $TlNO_3$ in 1/1 EtOH/H_2O was often used as a substitute for the ethanolic solution of $TlPF_6$ with negligible changes in the purity or yield of the product. Li{$(NDippCMe)_2CH$ (**6**) was prepared according to the literature procedure.[77]

Synthesis of "GaI". Note: we found it most reliable to prepare 500 mg of "GaI" at one time. The reaction can be scaled to prepare greater than 10 g of "GaI"; however, the reaction time must be adjusted accordingly.

Gallium metal (0.1863 g, 2.674 mmol, 1 equiv) was weighed into a 100 mL pressure tube in the glovebox. The gallium metal was heated until it melted and spread about the bottom of the flask in an effort to maximize surface area. Toluene (4.5 mL) was added, followed by iodine (0.3393 g, 1.337 mmol, 0.5 equiv). Residual iodine was rinsed with toluene (4.5 mL) and added to the reaction mixture, and the vessel was sealed with an O-ring fitted screw-thread Teflon stopper. The resulting purple solution was then sonicated at 30 °C in 20 min intervals for 40−120 min, with vigorous physical agitation between each interval. Toluene was removed in vacuo to yield a gray to green powder depending on the time. Yield: 100%, 0.525 g, 2.67 mmol.

FT-Raman spectroscopy (cm^{-1} (intensity normalized to 2)): 40 min sample, 267 (0.03), 230 (0.11), 213 (0.03), 141 (2), 124 (0.04), 86 (0.26); 60 min sample, 292 (0.02), 232 (0.06), 213 (0.05), 141 (2), 124 (0.43), 84 (0.30); 80 min sample, 292 (0.12), 232 (0.05), 213 (0.04), 188 (0.04), 141 (1.66), 124 (2), 84 (0.70); 100 min sample, 292 (0.12), 188 (0.04), 141 (0.04), 124 (2), 84 (0.49).

FT-Raman spectroscopy for other gallium iodides: GaI_2, 235 (w), 214 (w), 143 (vs);[43] Ga_2I_3, 292 (s), 186 (w), 124 (vs), 79 (m);[43] GaI_3, 267 (0.05), 227 (0.20), 194 (0.03), 163 (0.10), 142 (2.0), 85 (0.35).

Synthesis of the Gallium(II) Dimer $[Ph_2B(CH_2PPh_2)_2(GaI)]_2$ (3). A suspension of $Tl[Ph_2B(CH_2PPh_2)_2]$ (**1**; 0.7777 g, 1.013 mmol, 1 equiv) in THF (3 mL) was prepared. In a separate vial, further THF (3 mL) was added to "GaI" (0.3877 g, 1.972 mmol, 2 equiv; 40 min preparation time) to give a fluid gray-green slurry. This slurry was immediately added to the suspension of **1** and rinsed with 3 mL of THF, resulting in an immediate color change to bright orange. After the mixture was stirred for 5 min, solids were removed by centrifugation, yielding a colorless supernatant that was concentrated in vacuo to give an off-white powder. Sequential washes with diethyl ether (3 mL) and CH_3CN (2 × 3 mL) and further drying in vacuo to remove residual solvent yielded a white powder. Single crystals suitable for X-ray diffraction were grown by vapor diffusion of pentane into a THF solution. Yield: 48%, 0.3172 g, 0.2087 mmol. Mp: 176−177 °C dec. ^{1}H NMR (400 MHz, $CDCl_3$, 25 °C, δ): 1.94 (br, 4H), 2.36 (br, 4H), 6.74 (m, 16H), 6.93 (t, 8H, $^3J_{H-H}$ = 7.6 Hz), 6.99 (q, 12H, $^3J_{H-H}$ = 8.0 Hz), 7.13 (m, 16H), 7.19 (t, 4H, $^3J_{H-H}$ = 7.6 Hz), 7.29 (t, 4H,

dx.doi.org/10.1021/ic501139w | Inorg. Chem. 2014, 53, 9644−9656

$^3J_{H-H}$ = 7.6 Hz). $^{31}P\{^1H\}$ NMR (161.82 MHz, $CDCl_3$, 25 °C, δ): −1.75. $^{11}B\{^1H\}$ NMR (128.23 MHz, $CDCl_3$, 25 °C, δ): −13.2. $^{13}C\{^1H\}$ NMR (100.5 MHz, $CDCl_3$, 25 °C, δ): 17.5−18.5 (br), 122.8, 123.3, 126.4, 126.6, 128.0, 128.8, 130.7, 131.1, 131.1 (d, $^1J_{P-C}$ = 56.5 Hz), 132.3, 132.8, 132.9 (d, $^1J_{P-C}$ = 54.3 Hz), 133.5, 134.3, 159.5−162.0 (br). FT-IR (cm^{-1} (ranked intensity)): 476 (13), 492 (7), 507 (4), 691 (1), 736 (3), 867 (5), 932 (11), 1098 (6), 1136 (12), 1307 (15), 1435 (2), 1484 (8), 3005 (14), 3038 (10), 3057 (9). FT-Raman (cm^{-1} (ranked intensity)): 86 (4), 101 (3), 143 (2), 204 (11), 220 (9), 234 (12), 262 (13), 1001 (1), 1032 (8), 1099 (10), 1155 (15), 1586 (6), 2884 (14), 3041 (7), 3057 (5). Anal. Calcd (found): C, 60.05 (59.25); H, 4.51 (4.23).

Synthesis of Compound 4. Compound **4** was prepared by a method similar to that for **3** using the 40 min "GaI" sample and $[Li(THF)_2(P^iPr_2CH_2)_2BPh_2]$ (**2**); however, this compound could not be isolated in greater than 85% purity. ^1H NMR (400 MHz, C_6D_6, 25 °C, δ): 0.67 (dd, 6H, $^3J_{H-H}$ = 6.4 Hz, $^3J_{P-H}$ = 13.2 Hz), 0.80−0.95 (m, 12H), 1.13 (dd, 6H, $^3J_{H-H}$ = 6.8 Hz, $^3J_{P-H}$ = 13.2 Hz), 1.57 (br t, 2H), 2.05 (br t, 2H), 2.68−2.78 (br, 4H), 7.05 (t, 1H, $^3J_{H-H}$ = 7.6 Hz), 7.20 (t, 1H, $^3J_{H-H}$ = 7.2 Hz), 7.30 (t, 2H, $^3J_{H-H}$ = 7.2 Hz), 7.35 (t, 2H, $^3J_{H-H}$ = 8.0 Hz), 7.70 (d, 2H, $^3J_{H-H}$ = 7.6 Hz), 7.90 (d, 2H, $^3J_{H-H}$ = 7.6 Hz). $^{31}P\{^1H\}$ NMR (161.82 MHz, C_6D_6, 25 °C, δ): 21.5. $^{11}B\{^1H\}$ NMR (128.23 MHz, C_6D_6, 25 °C, δ): −13.0.

Synthesis of $[Li(THF)_4][GaI_3\text{-}GaI(P^iPr_2CH_2)_2BPh_2]$ (5). A solution of $[Li(THF)_2(P^iPr_2CH_2)_2BPh_2]$ (**2**; 57.9 mg, 0.10 mmol, 1.0 equiv) in THF (3 mL) was prepared. Separately, a vial was charged with "GaI" (40.0 mg, 0.20 mmol, 2.0 equiv; 100 min preparation time) followed by THF (3 mL) to give a suspension of green particles. The solution of **2** was immediately added to this suspension in a rapid dropwise fashion and the resulting mixture stirred for 5 min. Solids were removed by centrifugation, and the supernatant was concentrated to an off-white solid in vacuo. Washing this solid with Et_2O (3 × 3 mL) and further drying in vacuo yielded a white powder. Yield: 28%, 0.0387 g, 0.282 mmol. ^1H NMR (400 MHz, C_6D_6, 25 °C, δ): 0.85 (dd, 6H, $^3J_{H-H}$ = 6.8 Hz, $^3J_{P-H}$ = 14.6 Hz), 0.95 (dd, 6H, $^3J_{H-H}$ = 6.4 Hz, $^3J_{P-H}$ = 14.6 Hz), 1.15 (dd, 6H, $^3J_{H-H}$ = 7.0 Hz, $^3J_{P-H}$ = 16.0 Hz), 1.30−1.40 (overlapping signals, 22H), 1.60 (t, 2H, $^2J_{P-H}$ = 15.4 Hz), 1.95 (t, 2H, $^3J_{P-H}$ = 15.4 Hz), 2.40−2.60 (overlapping doublet of septets, 4H), 3.50 (t, 16H, $^3J_{H-H}$ = 6.4 Hz), 7.05 (t, 1H, $^3J_{H-H}$ = 7.6 Hz), 7.20 (t, 1H, $^3J_{H-H}$ = 8.0 Hz), 7.30 (t, 2H, $^3J_{H-H}$ = 7.2 Hz), 7.35 (t, 2H, $^3J_{H-H}$ = 7.6 Hz), 7.70 (d, 2H, $^3J_{H-H}$ = 7.2 Hz), 7.90 (d, 2H, $^3J_{H-H}$ = 8.0 Hz). $^{31}P\{^1H\}$ NMR (161.82 MHz, C_6D_6, 25 °C, δ): 17.9. $^{11}B\{^1H\}$ NMR (128.23 MHz, C_6D_6, 25 °C, δ): −13.4.

Reactions of "GaI" with $Li\{(NDippCMe)_2CH$ (6). A solution of **6** (49.5 mg, 0.118 mmol, 1 equiv) was prepared in 1.5 mL of benzene-d_6. Separately, a suspension of "GaI" (35.3 mg, 0.177 mmol, 1.5 equiv) in 1.5 mL of benzene-d_6 was prepared. The solution of **6** was added to the "GaI" suspension dropwise. After the mixture was stirred for 1 h, the crude suspension was filtered and a ^1H NMR spectrum obtained to characterize the product mixture.

■ ASSOCIATED CONTENT

Ⓢ Supporting Information

Text, figures, tables, and CIF files giving complete NMR spectral data, solid-state NMR spectral data, the solid-state structure of the potassium reduction product, and crystallographic data for **3**−**5** and the the potassium reduction product. This material is available free of charge via the Internet at http://pubs.acs.org.

■ AUTHOR INFORMATION

Corresponding Author

*E-mail for P.J.R.: pragogna@uwo.ca.

Notes

The authors declare no competing financial interest.

■ ACKNOWLEDGMENTS

We thank the Natural Science and Engineering Research Council of Canada (NSERC), the Ontario Government, the Canadian Foundation of Innovation (CFI), and The University of Western Ontario for their generous funding. Prof. Robert Schurko from the University of Windsor is thanked for sending us the code for the WURST-QCPMG pulse sequence.

■ REFERENCES

(1) Power, P. P. *Nature* **2010**, *463*, 171.
(2) Power, P. P. *Acc. Chem. Res.* **2011**, *44*, 627.
(3) Schmidt, E. S.; Jockisch, A.; Schmidbaur, H. *J. Am. Chem. Soc.* **1999**, *1*, 9758.
(4) Asay, M.; Jones, C.; Driess, M. *Chem. Rev.* **2010**, *111*, 354.
(5) Baker, R. J.; Farley, R. D.; Jones, C.; Kloth, M.; Murphy, D. M. *J. Chem. Soc., Dalton Trans.* **2002**, 3844.
(6) Hardman, N. J.; Eichler, B. E.; Power, P. P. *Chem. Commun.* **2000**, *53*, 1991.
(7) Jones, C.; Junk, P. C.; Platts, J. A.; Stasch, A. *J. Am. Chem. Soc.* **2006**, *128*, 2206.
(8) Jones, C.; Mills, D. P.; Platts, J. A.; Rose, R. P. *Inorg. Chem.* **2006**, *45*, 3146.
(9) Green, S. P.; Jones, C.; Stasch, A. *Inorg. Chem.* **2007**, *46*, 11.
(10) Baker, R. J.; Jones, C.; Platts, J. A. *J. Am. Chem. Soc.* **2003**, *125*, 10534.
(11) Arnold, P. L.; Liddle, S. T.; McMaster, J.; Jones, C.; Mills, D. P. *J. Am. Chem. Soc.* **2007**, *129*, 5360.
(12) Green, S. P.; Jones, C.; Mills, D. P.; Stasch, A. *Organometallics* **2007**, *26*, 3424.
(13) Bonello, O.; Jones, C.; Stasch, A.; Woodul, W. D. *Organometallics* **2010**, *29*, 4914.
(14) Burford, N.; Ragogna, P. J.; Robertson, K. N.; Cameron, T. S.; Hardman, N. J.; Power, P. P. *J. Am. Chem. Soc.* **2001**, *124*, 382.
(15) Lichtenthaler, M. R.; Higelin, A.; Kraft, A.; Hughes, S.; Steffani, A.; Plattner, D. A.; Slattery, J. M.; Krossing, I. *Organometallics* **2013**, *32*, 6725.
(16) Higelin, A.; Sachs, U.; Keller, S.; Krossing, I. *Chem. Eur. J.* **2012**, *18*, 10029.
(17) Higelin, A.; Haber, C.; Meier, S.; Krossing, I. *Dalton Trans.* **2012**, *41*, 12011.
(18) Higelin, A.; Keller, S.; Göhringer, C.; Jones, C.; Krossing, I. *Angew. Chem., Int. Ed.* **2013**, *52*, 4941.
(19) Slattery, J. M.; Higelin, A.; Bayer, T.; Krossing, I. *Angew. Chem., Int. Ed.* **2010**, *49*, 3228.
(20) Wehmschulte, R. J. *Angew. Chem., Int. Ed.* **2010**, *49*, 4708.
(21) Fedushkin, I. L.; Nikipelov, A. S.; Lyssenko, K. A. *J. Am. Chem. Soc.* **2010**, *132*, 7874.
(22) Fedushkin, I. L.; Nikipelov, A. S.; Morozov, A. G.; Skatova, A. A.; Cherkasov, A. V.; Abakumov, G. A. *Chem.—Eur. J.* **2012**, *18*, 255.
(23) Cooper, B. F. T.; Macdonald, C. L. B. Mixed Valent Compounds of Al, Ga, In and Tl. In *The Group 13 Metals Aluminium, Gallium, Indium and Thallium. Chemical Patterns and Peculiarities*,; Aldridge, S., Downs, A. J., Eds.; Wiley: Chichester, U.K., 2011.
(24) Jones, C.; Stasch, A. The Chemistry of the Group 13 Metals in the +1 Oxidation State. In *The Group 13 Metals Aluminium, Gallium, Indium and Thallium. Chemical Patterns and Peculiarities*; Aldridge, S., Downs, A. J., Eds.; Wiley: Chichester, U.K., 2011.
(25) Baker, R. J.; Jones, C. *Dalton Trans.* **2005**, 1341.
(26) Green, M. L. H.; Mountford, P.; Smout, G. J.; Speel, S. R. *Polyhedron* **1990**, *9*, 2763.
(27) There have been considerable efforts in the synthesis of gallium−iodine phases in varying stoichiometries, including a 1:1 phase that could be considered a type of "GaI", prior to Green's report. For a brief description of this history and the appropriate citations, see the Supporting Information.
(28) Coban, S. Diplomarbeit; Universitat Karlsruhe, Karlsruhe, Germany, 1999.

(29) Widdifield, C. M.; Jurca, T.; Richeson, D. S.; Bryce, D. L. *Polyhedron* **2012**, *35*, 96.
(30) Doriat, C. U.; Friesen, M.; Baum, E.; Ecker, A.; Schnockel, H. *Angew. Chem., Int. Ed.* **1997**, 1969.
(31) Schnepf, A.; Doriat, C.; Mollhausen, E.; Schnöckel, H. *Chem. Commun.* **1997**, *0*, 2111.
(32) Cheng, F.; Hector, A. L.; Levason, W.; Reid, G.; Webster, M.; Zhang, W. *Inorg. Chem.* **2007**, *46*, 7215.
(33) Thomas, J. C.; Peters, J. C. *Inorg. Chem.* **2003**, *42*, 5055.
(34) Mankad, N. P.; Antholine, W. E.; Szilagyi, R. K.; Peters, J. C. *J. Am. Chem. Soc.* **2009**, *131*, 3878.
(35) Thomas, J. C.; Peters, J. C. *J. Am. Chem. Soc.* **2001**, *123*, 5100.
(36) Lu, C. C.; Peters, J. C. *J. Am. Chem. Soc.* **2002**, *124*, 5272.
(37) Thomas, J. C.; Peters, J. C. *J. Am. Chem. Soc.* **2003**, *125*, 8870.
(38) Dube, J. W.; Macdonald, C. L. B.; Ragogna, P. J. *Angew. Chem., Int. Ed.* **2012**, *124*, 13203.
(39) Weicker, S. A.; Dube, J. W.; Ragogna, P. J. *Organometallics* **2013**, *32*, 6681.
(40) Dube, J. W.; Ragogna, P. J. *Chem.—Eur. J.* **2013**, *19*, 11768.
(41) Dube, J. W.; Macdonald, C. L. B.; Ellis, B. D.; Ragogna, P. J. *Inorg. Chem.* **2013**, *52*, 11438.
(42) Gerlach, V. G.; Honle, W.; Simon, A. *Z. Anorg. Allg. Chem.* **1982**, *486*, 7.
(43) Beamish, J. C.; Wilkinson, M.; Worrall, I. J. *Inorg. Chem.* **1978**, *17*, 2026.
(44) Lind, W.; Worrall, I. J. *J. Organomet. Chem.* **1972**, *40*, 35.
(45) Lind, W.; Waterworth, L.; Worrall, I. J. *Inorg. Nucl. Chem. Lett.* **1971**, *7*, 611.
(46) Waterworth, L. G.; Worrall, I. J. *J. Inorg. Nucl. Chem.* **1973**, *35*, 1535.
(47) Wilkinson, M.; Worrall, I. J. *J. Organomet. Chem.* **1975**, *93*, 39.
(48) Woodward, L. A.; Singer, G. H. *J. Chem. Soc.* **1958**, 716.
(49) Tan, K. H.; Taylor, M. J. *Inorg. Nucl. Chem. Lett.* **1974**, *10*, 267.
(50) Evans, C. A.; Taylor, M. J. *J. Chem. Soc. D Chem. Commun.* **1969**, 1201.
(51) ^{127}I nuclear quadrupole resonance (NQR) spectroscopy is an ideal technique to study "GaI", because each crystallographically unique I atom will give rise to a peak at a specific transmitter frequency. Since there are four crystallographically unique I atoms in the $[GaI_4^-]$ component of GaI_2 and three distinct I types in the $[Ga_2I_6^{2-}]$ component of Ga_2I_3, ^{127}I NQR is able to unambiguously differentiate between the two species. Previous studies on GaI_2[52] and GaI_3,[53] show the range of frequencies to be from 113.6 to 174.6 MHz, which conveniently fall within the standard tuning range of our NMR probes and are thus easily accessible. Although it is possible to use solid-state ^{127}I NMR to study "GaI", each distinct I site will give rise to a broad powder pattern spanning many megahertz.[54] The unique I sites in "GaI" will thus overlap and make it difficult to unambiguously identify the number of unique I sites present in a "GaI" sample. The advantage of ^{127}I NQR over ^{127}I ssNMR is that, even though the NQR peaks are relatively broad (line widths of a few hundred kilohertz) and featureless, they are spread over a broad frequency range and typically do not overlap.
(52) Okuda, T.; Hamamoto, H.; Ishihara, H.; Negita, H. *Bull. Chem. Soc. Jpn.* **1985**, *58*, 2731.
(53) Segel, S. L.; Barnes, R. G. *J. Chem. Phys.* **1956**, *25*, 578.
(54) Widdifield, C. M.; Chapman, R. P.; Bryce, D. L. In *Annual Reports on NMR Spectroscopy*; Webb, G. A., Ed.; Elsevier: San Diego, CA, 2009; Vol. *66*, pp 195−326.
(55) Buslaev, Y. A.; Tarasov, V. P.; Petrosyants, S. P.; Melnikov, N. N. *Zh. Strukt. Khim.* **1974**, *15*, 617.
(56) QCPMG NMR spectra are comprised of spikelets that mimic the overall shape of the spin-echo powder pattern but provide a dramatic signal enhancement in comparison to typical spin-echo experiments: Larsen, F. H.; Jakobsen, H. J.; Ellis, P. D.; Nielsen, N. C. *J. Phys. Chem. A* **1997**, *101*, 8597.
(57) It has been shown that when QCPMG is combined with adiabatic WURST pulses, dramatic increases in the excitation bandwidth of the QCPMG experiment is achieved and broad powder patterns can be obtained much more efficiently than when traditional procedures are used: O'Dell, L. A.; Schurko, R. W. *Chem. Phys. Lett.* **2008**, *464*, 97−102.
(58) *Multinuclear NMR*; Mason, J., Ed.; Plenum Press: New York and London, 1987.
(59) McGarvey, B. R.; Talyor, M. J.; Tuck, D. J. *Inorg. Chem.* **1981**, *20*, 2010.
(60) Antcliff, K. L.; Baker, R. J.; Jones, C.; Murphy, D. M.; Rose, R. P. *Inorg. Chem.* **2005**, *44*, 2098.
(61) Beamish, J. C.; Boardman, A.; Worrall, I. J. *Polyhedron* **1991**, *10*, 95.
(62) Ali, S. M.; Brewer, F. M.; Chadwick, J. R.; Garton, G. *J. Inorg. Nucl. Chem.* **1959**, *9*, 124.
(63) Brewer, F. M.; Chadwick, J. R.; Garton, G. *J. Inorg. Nucl. Chem.* **1961**, *23*, 45.
(64) Tuck, D. G. *Polyhedron* **1990**, *9*, 377.
(65) Arif, A. M.; Benac, B. L.; Cowley, A. H.; Geerts, R.; Jones, R. A.; Kidd, K. B.; John, M.; Schwab, S. T. *J. Chem. Soc., Chem. Commun.* **1986**, *1543*, 1543.
(66) Petrie, M. A.; Power, P. P. *Organometallics* **1993**, *12*, 1592.
(67) Gans-Eischler, T.; Jones, C.; Aldridge, S.; Stasch, A. *Anal. Sci.* **2008**, *24*, 109.
(68) *SMART*; Bruker AXS Inc., Madison, WI, USA, 2001.
(69) *COLLECT*; Nonius BV, Delft, The Netherlands, 2001.
(70) *SAINT*; Bruker AXS Inc., Madison, WI, USA, 2007.
(71) *SADABS*; Bruker AXS Inc.: Madison, WI, USA, 2001.
(72) Sheldrick, G. M. *Acta Crystallogr., Sect. A* **2008**, *64*, 112.
(73) Eichele, K. WSolids, 2013; http://casgm3.anorg.chemie.uni-tuebingen.de/klaus/soft/index.php?p=wsolids1/wsolids1.
(74) Cheng, J. T.; Edwards, J. C.; Ellis, P. D. *J. Phys. Chem.* **1990**, *94*, 553.
(75) Power, W. P.; Wasylishen, R. E.; Mooibroek, S.; Pettitt, B. A.; Danchura, W. *J. Phys. Chem.* **1990**, *94*, 591.
(76) Mason, J. *Solid State Nucl. Magn. Reson.* **1993**, *2*, 285.
(77) Stender, M.; Wright, R. J.; Eichler, B. E.; Prust, J.; Olmstead, M. M.; Roesky, H. W.; Power, P. P. *J. Chem. Soc., Dalton Trans.* **2001**, 3465.